DIFFUSION OF MOLECULES ON BIOLOGICAL MEMBRANES OF NONPLANAR FORM

A Theoretical Study

BORIS M. AIZENBUD
Chemistry Department, Ben Gurion University, Beer Sheva, Israel

NAHUM D. GERSHON
Physical Sciences Laboratory, Division of Computer Research and Technology, National Institutes of Health, Bethesda, Maryland 20205

ABSTRACT Lateral mobility of molecules on cell membranes has been recently studied by fluorescence photobleaching recovery (FPR) techniques. The interpretation of these results in terms of diffusion along the membranes is based on the assumption that the surface is planar, although biological membranes may have blebs and microvilli. To study the effect of nonplanarity on the diffusion rate, the diffusion equation along curved surfaces was derived and was solved numerically for a "wavy" surface of the form $A \cos kx \cos ky$. Calculations show that for $k=10\pi$ μm^{-1} and a bleached spot of 1 μm in diameter, the time dependence of the intensity of fluorescence in the bleached spot depends on A at $A<0.5$ μm, while at higher values of A (1 and 2 μm) the dependence is weak. If one calculates diffusion coefficients from FPR measurements and assumes that the membrane is planar, the resulting diffusion coefficient is not less than about half of the real one. Because of the tortuous shape of the spot boundary, increasing the microvilli length from 0.5 μm to 1 or 2 μm does not change the diffusion rates. These considerations are valid for times when the diffusion is dominated by molecules that were initially located close to the spot boundary.

INTRODUCTION

It has been demonstrated in recent years that molecules can move laterally on biological membranes. This phenomenon was first observed by Frye and Edidin (1) by fusing two cells, each having a differently labeled surface molecule; the mobile molecules from the two different cells mixed with each other (heterokaryon method) and a diffusion constant was calculated from the rate of mixing (2, 3). An additional demonstration of the possible mobility of molecules on cell surfaces was the experiment performed by Taylor et al. (4) in which cell receptors were capped. By cross-linking membrane receptors by multivalent ligands it first was possible to aggregate the cross-linked mobile molecules into patches and then into one region (a "cap").

A more quantitative approach involving fluorescence photobleaching recovery (FPR) was developed later (5–9). In these experiments, either naturally or artificially marked fluorescent molecules are probed. Using laser light, a small area on the membrane (usually with a diameter of 1 μm) is bleached. Bleached molecules move out of the area in which they were initially located and unbleached molecules move into the bleached area. From the measured fluorescence intensity in the bleached spot, at different times a diffusion constant is calculated. Application of the FPR method to study diffusion in planar membranes, at least from the theoretical point of view, is clear. An analytical solution of the diffusion equation on a plane with a circular bleached stain as the initial condition can be found, even if the bleaching time cannot be neglected. The difficulty is, however, that in many cases biological membranes are not planar, but have blebs and microvilli. In such cases, diffusion constants measured by FPR represent mobility on projected flat planes of real nonflat membranes.

The purpose of this work is to discuss the effect of surface curvature on the observed diffusional motion of molecules. The motion of single molecules along a membrane should not of course be affected by the topography of the surface, as long as the curvature does not change the intermolecular interactions. But, as is expressed in the following sections, we seldom look at the diffusion of single molecules but, rather, at changes of composition in macroscopic areas that contain many molecules. Such macroscopic areas are, for example, the bleached spot in fluorescence photobleaching recovery

Dr. Aizenbud's present address is the Massachusetts Institute of Technology, Department of Chemistry, Cambridge, Massachusetts 02139

measurements or areas on membranes that have a momentarily different composition than the rest of the cell surface (e.g., after fusion with an endogeneous or exogeneous vesicle). The diffusion of molecules in and out of macroscopic areas is affected not only by the shape of the area but also by the form and length of its boundary. These effects are studied in the next sections.

In the accompanying paper, Wolf et al. (10) present FPR measurements of the diffusion of a lipid analogue. They found that the rate of fluorescence recovery is similar in microvillous surfaces and in those that have much smaller protuberances. As discussed in the Discussion section, these results seem to agree with the present theoretical analysis, which was performed independently (see also reference 11).

DIFFUSION IN CURVED MEMBRANES

In this section we present a mathematical description of diffusion along curved surfaces, based on a diffusion equation. This equation is solved for a simple "wavy" curved surface, which can represent a membrane with microvilli. Numerical results that describe the disappearance of tagged molecules from a patch with a circular projection on the xy plane are given at the end of this section.

The first step in the calculation is the determination of the diffusion equation along a curved surface. The curved surface can be represented by $z = f(x,y)$. The resulting diffusion equation for this surface is (for the derivation see Appendix I)

$$\begin{aligned}\frac{\partial C}{\partial t} = D\Bigg(&\Bigg\{\frac{\partial^2 C}{\partial x^2}\left[1+\left(\frac{\partial f}{\partial y}\right)^2\right]+\frac{\partial^2 C}{\partial y^2}\left[1+\left(\frac{\partial f}{\partial x}\right)^2\right]\\&-2\frac{\partial^2 C}{\partial x\partial y}\frac{\partial f}{\partial x}\frac{\partial f}{\partial y}\Bigg\}\Big/R^2\\&-\frac{\partial C}{\partial x}\Bigg\{\frac{\partial^2 f}{\partial x^2}\frac{\partial f}{\partial x}\left[1+\left(\frac{\partial f}{\partial y}\right)^2\right]+\frac{\partial^2 f}{\partial y^2}\frac{\partial f}{\partial x}\left[1+\left(\frac{\partial f}{\partial x}\right)^2\right]\\&-\frac{\partial^2 f}{\partial x\partial y}\left[2\frac{\partial f}{\partial y}\left(\frac{\partial f}{\partial x}\right)^2\right]\Bigg\}\Big/R^4\\&-\frac{\partial C}{\partial y}\Bigg\{\frac{\partial^2 f}{\partial x^2}\frac{\partial f}{\partial y}\left[1+\left(\frac{\partial f}{\partial y}\right)^2\right]+\frac{\partial^2 f}{\partial y^2}\frac{\partial f}{\partial y}\left[1+\left(\frac{\partial f}{\partial x}\right)^2\right]\\&-\frac{\partial^2 f}{\partial x\partial y}\left[2\frac{\partial f}{\partial x}\left(\frac{\partial f}{\partial y}\right)^2\right]\Bigg\}\Big/R^4\Bigg),\end{aligned}\tag{2.1}$$

where $\partial f/\partial x \equiv f_x$ means partial derivative with respect to x, etc., and

$$R = (1 + f_x^2 + f_y^2)^{1/2}.\tag{2.2}$$

If the surface is planar, i.e., $\partial f/\partial x = \partial f/\partial y = 0$ the diffusion equation along a plane is obtained (see Appendix I).

To solve this diffusion equation it is necessary to specify the shape of the surface along which the molecules are moving. Cell membranes usually have blebs and microvilli, and specifying their exact mathematical shape is a formidable task. Therefore we choose a surface which is mathematically simple but has a structure which should resemble microvillous membranes,

$$z = A\cos kx\cos ky,\tag{2.3}$$

where A is the amplitude and k is the wavenumber (2π/wavelength). This surface is periodic along x and y and is similar to the surface of an egg carton (see Fig. 1 *A*). It is a square lattice of microvilli, but when rotated by 45° (see Fig. 1 *B*) it looks like a distorted hexagonal lattice. Initially the surface is covered with a uniform distribution of tagged molecules. These molecules move randomly on the plane of the membrane. Macroscopic areas contain many molecules whose movement is described by the diffusion equation (Eq. 2.1). We considered an area that has a circular projection on the xy plane with a radius of 0.5 μm. Assuming that we can tag the molecules that are initially confined to this spot (e.g., by bleaching the fluorescent markers attached to them) it is possible to study their diffusion out from this circular area (the "bleached spot"). By solving the diffusion equation (Eq. 2.1) for the situation in

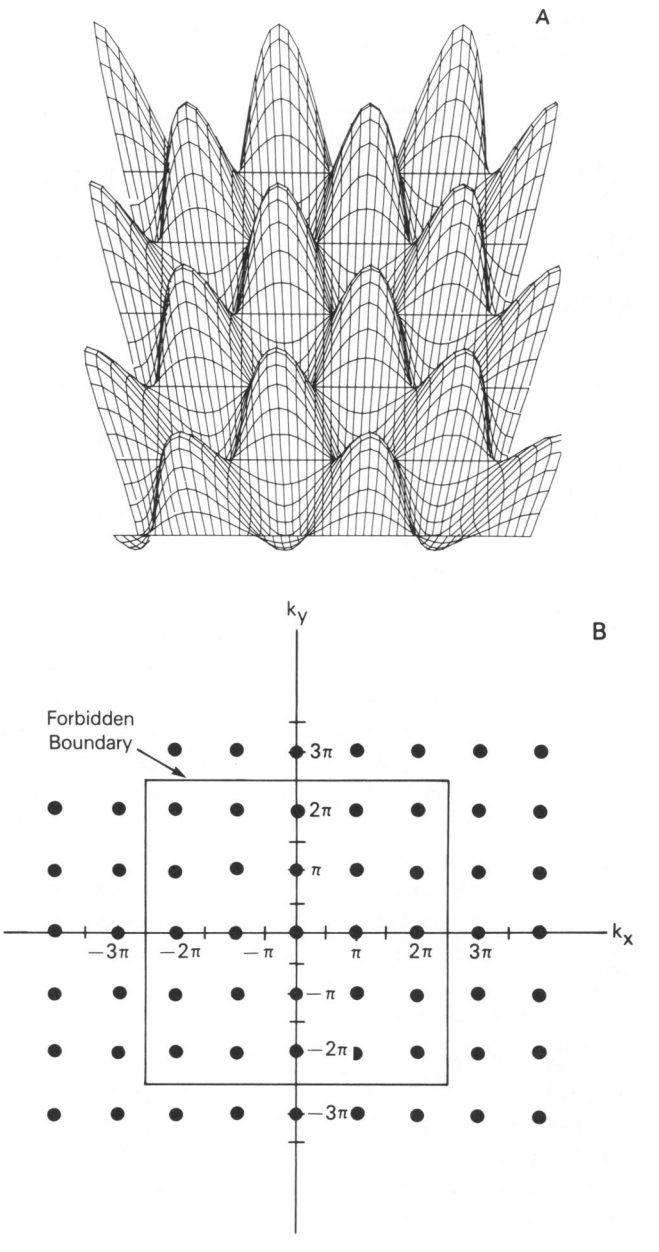

FIGURE 1 *A* A two-dimensional representation of the surface $z = A\cos kx\cos ky$ (e.g., Eq. 2.3) for $A = 0.75$ μm $k = 2\pi/(0.2$ μm). This figure was generated by G. Knott using the MLAB program (12) at the computer facilities of the National Institutes of Health, Bethesda, MD. *B*, the locations of the microvilli's peaks of the system represented in Fig. 1 *A*. The forbidden boundary passes through points in which the value of z is 0.

which the molecules inside the circular spot are bleached at time zero, in other words, with the initial conditions

$$C(x,y) = \begin{cases} C_0 & x^2 + y^2 \le r_0^2 \\ 0 & x^2 + y^2 > r_0^2, \end{cases} \tag{2.4}$$

we obtained the number of the bleached molecules still remaining in the spot at subsequent times. This number is given by the following expression:

$$J(t) = \iint C(x,y,t)[1 + (\partial f/\partial x)^2 + (\partial f/\partial y)^2]^{1/2} dx dy \qquad x^2 + y^2 \le r_0^2. \tag{2.5}$$

The diffusion equation was solved numerically. A numerical solution, as described in Appendix II, is not continuous in time and space. The concentration of bleached molecules is given for points in the x,y plane separated by $1/60$ μm and for time intervals, Δt, of 6.94×10^{-3} s for $D = 10^{-10}$cm^2/s. The calculation was carried out for $k = 10\pi$ μm^{-1} which corresponds to 0.1 μm thick microvilli.

The solutions were then integrated over a circular spot of 1 μm in diameter to yield the number of bleached molecules in this spot at different times (0, Δt, $2\Delta t$, $3\Delta t$, . . .). This number, divided by the number of bleached molecules in the spot at time 0, yields the fractional concentration of the tagged particles in the circular spot. We call this entity $J(t)/J(0)$.

The fractional concentrations of the tagged particles within the spot were calculated for several membrane topographies. For a planar membrane for which the amplitude of the surface, A, is zero, the fractional concentration was calculated for 1,550 time intervals (up to $6.94 \times 10^{-3} \times 1{,}550$ s for $D = 10^{-10}$ cm^2/s). For curved membranes of different amplitudes (which have the same number of microvilli per unit area but with different lengths) e.g., $A = 0.1$, 0.5, and 2 μm, the fractional concentration was calculated for 250 time intervals. In addition, the calculation was carried out for 3,533 time intervals for the case where $A = 1$ μm. The calculations were performed in a CDC-CYBER computer (Control Data Corp., Minneapolis, MN) and took 100 h CPU time.

The results of these fractional concentrations are given in Fig. 2 for the first 250 time intervals. It is evident from Fig. 2 that the rate of disappearance of bleached molecules from the circular region, in which they were originally located, depends strongly on the shape of the membrane for planar membranes (A=0) or ones with short microvilli ($0<A<0.5$ μm). This rate of disappearance is almost independent of the shape of the membrane for intermediate and long microvilli (amplitudes >0.5 μm). The curve describing the disappearance of the bleached molecules on a membrane with $A = 5$ μm is situated nearer to the curve with $A=10$ μm than to the curve with $A=2$ μm.

We also examined the possible effects on the diffusion coefficient computed by considering a microvillous membrane to be flat. The reason for this calculation is that in the interpretation of the measurements of the FPR experiments in terms of diffusion along a membrane, the membrane surface is considered to be flat. We calculated the value of the diffusion constant that will bring a disappearance curve for a microvillous membrane with an amplitude of $A=1$ μm into correspondence with a curve for diffusion on a planar membrane. The results are presented in Fig. 3. It is evident that for this case considering the microvillous membrane to be flat introduces a diffusion constant that is 2–2.5 times smaller than the calculated diffusion constant.

The results presented in this section represent calculations for 250–3,533 time steps. Computations for longer times require much more expensive computer time. The conclusions that can be drawn for later times beyond the present calculations are discussed in the next section.

DISCUSSION

The macroscopic topography of the surface should not influence the motion of single molecules if the diffusion constant remains the same (i.e., no restrictions are added to the molecular dynamics by bending of the membrane or by changes in the membrane composition that may be required to make the surface curved). But changing the membrane topography, e.g., from a flat membrane to a membrane with macroscopic blebs, can change the rates of diffusion in and out of macroscopic areas. This may result from interference with the dynamics of single molecules, but also by changes in the boundary conditions necessary

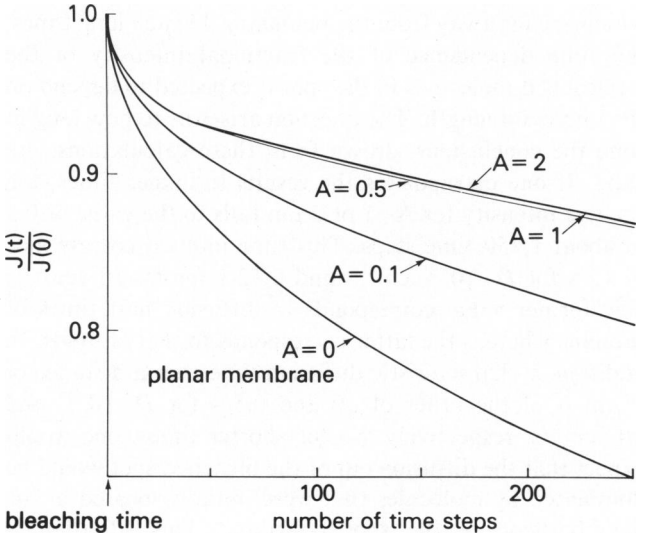

FIGURE 2 Fractional concentration of tagged molecules originally in the circular spot at time $t=0$ as a function of time for different surface topographies (length of microvilli $A = 0$, 0.1, 0.5, 1, and 2 μm). One time step is 6.94×10^{-3} s.

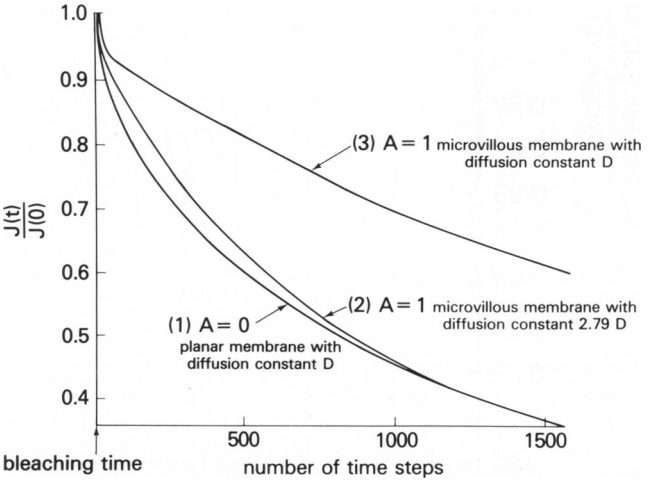

FIGURE 3 The effect of taking the membrane as planar on the measured diffusion coefficient. Fractional concentration of tagged molecules originally in the circular spot at time $t=0$ as a function of time for $A=1$ μm (curve *1*) and for a planar membrane $A = 0$ (curve *3*) having the same diffusion coefficient are presented in this figure. Curve *2* is for the same topography as curve *1* ($A=1$ μm) but with a different diffusion coefficient ($2.79D$) so as to match more or less the planar case (curve *1*).

for solving the diffusion equation. In the last section the effects of changes in the amplitude (or in other words, the length of the microvilli) were calculated. When the length of the microvilli is increased, the area of the membrane enclosed in the circular bleached spot is increased by the same factor. This can be easily seen if one considers a microvillus to have an approximate shape of a cone. Keeping the base fixed, the upper surface area of a cone depends in a linear fashion on its height (A, the microvillus length). When the length of the microvilli, or A, is changed, not only is the area of the membrane enclosed in the circular bleached spot increases, but the length of the boundary between the spot and the rest of the surface increases concomitantly. If this happens, the molecules that were originally in this area would have more ways to leave, and the outside molecules would have more chance to enter through the elongated boundary. The ratio between the area of the circular spot on the surface $A \cos kx \cos ky$ and its boundary length is given in Fig. 4 for $k=10\pi\ \mu m^{-1}$. The length of the boundary of the circular spot and its area are nonlinear with A at low values of A (up to $A=0.3\ \mu m$) and then become linear. Thus, at large values of the amplitude, $A>>2\pi/k$, the spot surface area and its boundary length are both linearly proportional to A. Similar behavior was found for $k=20\pi\ \mu m^{-1}$, where this ratio reaches a constant value of 0.36 already at $A=0.2\ \mu m$. In the system analyzed here, with the characteristic dimensions close to those of natural situations, a large number of the microvilli are intersected by the spot boundary. Under these conditions an increase in A would not result in much change in the diffusion rate of molecules to and from the bleached area, at least for times when the diffusion flow consists mainly of bleached molecules that were initially located close to the boundary.

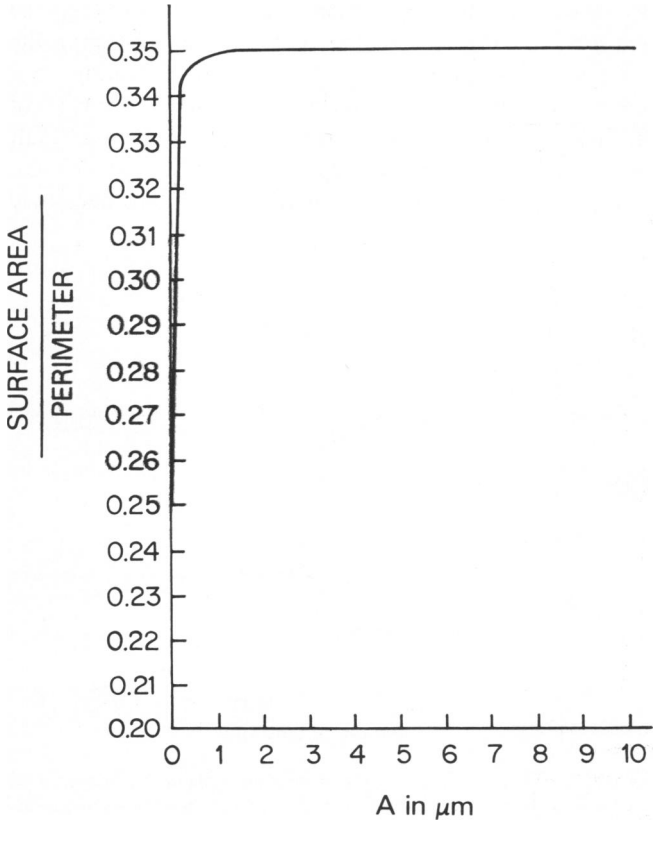

FIGURE 4 The A dependence of the ratio of the spot area and the spot perimeter for a spot on a surface $z = A \cos kx \cos ky$ having a projected circular shape in the xy plane.

The observation illustrated in Fig. 4, namely, that the ratio of the length of the boundary of the bleached spot to its area reaches a constant value for long microvilli, is valid for other surfaces. In Appendix III, we show that the preceding statement holds for surfaces that can be mathematically described by an expression that is of the form of A times a function of x and y and which has the following two features. The first characteristic is that most of the areas contained in the spot are not parallel to the xy plane. The second feature is that most of the spot boundary has lines that are not parallel to the xy plane. (These properties are rigorously described in Appendix III). Thus, for such surfaces with long microvilli, the time dependence of the fractional concentration of the bleached molecules is expected not to depend strongly on the microvilli length; at least for the lengths and the times considered in these calculations.

The calculations presented here are performed for a specified length of time because of computing cost limitations. For very long periods after the initial bleach, one expects to encounter a situation where the diffusion of molecules initially located near the boundary of the bleached spot becomes relatively unimportant as compared with the diffusion from regions deep in the spot, which are far away from the boundary. In such long times, the time dependence of the fractional intensity of the unbleached molecules in the spot is expected to depend on the microvilli length. The question arises as to how long in time the conclusions, drawn from these calculations, are valid. If one extrapolates the results to longer times, the relative intensity for A=1 or 2 μm falls to the value of 0.5 in about 1,750 time steps. This time interval corresponds to 12 s for $D=10^{-10}$ cm^2/s and 0.12 s for $D=10^{-8}$cm^2/s. The former value corresponds to diffusion half times of proteins whereas the latter corresponds to that of lipids. In addition, a characteristic diffusion time over a distance of 1 μm is of the order of 50 and 0.5 s for $D=10^{-10}$ and 10^{-8}cm^2/s, respectively. So for shorter times, one would expect that the diffusion out of the bleached spot would be dominated by molecules that were initially located in the neighborhood of the spot boundary. This situation is anticipated to be valid in many experiments where the diffusion constant is calculated from the time in which the intensity of the bleached molecules in the spot decays into

half of its initial value. These statements should be in effect for larger microvilli lengths as long as about half of the bleached molecules can diffuse out in the times considered above. We would like to point out that this analysis does not exclude the possibility that changes in surface topography might contribute to changes at the immobile fraction (at extremely long times).

It is interesting to compare this two-dimensional case with diffusion of molecules along a line (one dimension) represented by $z=A\cos kx$. The spot on which our attention is focused is, for example, a line on the x axis from $x=-0.5$ μm to $x=+0.5$ μm. Molecules can diffuse in and out of this spot by crossing the two points ($x=+0.5$ and -0.5 μm). When the length of the one-dimensional microvilli, A, is changed the length of the membraneous line, contained in the spot, is changed accordingly, but the boundary between the spot and the rest of the membrane is unchanged. Thus, in contrast with the two-dimensional case considered here, in one dimension the rate of diffusion of molecules in and out of the spot will decrease as A increases.

Recently, Dragsten et al. (13) have found little or no difference in the rate of photobleaching recovery of lipid probe molecules in lymphocytes with or without microvilli. In the accompanying paper, Wolf et al. (10) present data on the diffusion of a lipid analogue on mouse egg surfaces. These cells have two types of surfaces: About two-thirds of the cell is microvillous and the remainder, as seen on the scanning electron microscopy level of resolution, appears to be smooth, as shown by Eager et al. (14). They found that the rate of diffusion is similar in both types of surfaces. If the surfaces described as devoid of microvilli have small protuberances (as was shown in a transmission electronmicrograph in reference 14), which cannot be seen at the scanning electron microscopy level, then those results seem to be compatible with the present theoretical calculations, which were performed independently (see reference 11).

To sum up, in this work we derived a diffusion equation for curved surfaces and calculated the fluorescence photobleaching recovery vs. time for a model surface of $A\cos kx\cos ky$ ($k=10\pi$ μm^{-1}). We arrived at the following conclusions: (*a*) If we consider a surface with microvilli of length 1 μm to be planar then the resulting diffusion coefficient is found to be not less than about half of that of a planar surface, although the microvillous surface can be as much as 21 times larger than the flat one. (*b*) Because of the tortuous shape of the spot boundary, changing the length of the microvilli from small (0.5 μm) to longer ones (1, 2 μm) does not change the rate in which the bleached molecules leave the spot. (*c*) These considerations are valid for short times, i.e., when the diffusion out of the bleached spot is dominated by molecules that were initially located in the neighborhood of the spot boundary. (*d*) These calculations may represent experimental situations where the diffusion coefficient is calculated from the half decay time, as is usually done in spot FPR.

APPENDIX I

Diffusion on a Curved Surface

In this Appendix we derive the diffusion equation on a curved surface. Let us consider a surface $z=f(x,y)$ in three-dimensional Euclidean space with Cartesian coordinates x, y, z, and let S be some arbitrary part of this surface, bounded by closed curve Γ. We assume, that surface $f(x,y)$ and curve Γ are smooth enough for our further calculations.

We can write the equations of curve Γ as follows:

$$\begin{aligned} x &= x(s) \\ y &= y(s) \\ z &= f[x(s), y(s)] = \eta(s), \end{aligned} \tag{I.1}$$

where, by s, we mean a natural parameter of Γ; i.e., the length of Γ from some arbitrary, but fixed point.

Now we introduce three important vector fields: τ^0, a unit vector, tangent to curve Γ; $\mathbf{m}^0$, a unit vector, normal to surface $z=f(x,y)$; $\mathbf{n}^0$, a unit vector, normal to curve Γ and tangent in the surface $z=f(x,y)$.

It can be easily seen, that these vectors have the following coordinate representation in each point:

$$\begin{aligned} \tau^0 &= (x_s, y_s, f_x x_s + f_y y_s) \\ \mathbf{m}^0 &= (f_x/R, f_y/R, -1/R) \\ \mathbf{n}^0 &= \tau^0 \times \mathrm{m}^0 \\ &= \{(y_s + f_y f_x x_s + f_y^2 y_s)/R, \\ &\quad -(x_s + f_x^2 x_s + f_x f_y y_s)/R, \\ &\quad (f_x y_s - f_y x_s)/R\} \end{aligned} \tag{I.2}$$

where

$$R = (1 + f_x^2 + f_y^2)^{1/2}. \tag{I.3}$$

If some substance, distributed on a surface $z=f(x,y)$ [we describe this distribution by the concentration $C(x,y,t)$], can be transported only by a diffusion mechanism, the conservation of mass equation has the following form:

$$(\partial/\partial t)\int_S\int C(x,y,t)\mathrm{d}s = -\ (\text{diffusion flow}). \tag{I.4}$$

The left-hand side of Eq. 2.4 can be rewritten as follows:

$$\frac{\partial}{\partial t}\int_S\int C(x,y,t)\,\mathrm{d}s = \int_{S'}\int \frac{\partial C(x,y,t)}{\partial t} R\,\mathrm{d}x\mathrm{d}y, \tag{I.5}$$

where S' is the projection of S on the xy plane. At the same time

$$\begin{aligned} (\text{diffusion flow}) &= \oint_\Gamma [-D\ \mathrm{grad}\ C(x,y,t), n^0]\mathrm{d}\Gamma \\ &= -\oint_{\Gamma'} P\,\mathrm{d}x + Q\,\mathrm{d}y, \end{aligned} \tag{I.6}$$

where D is the diffusion coefficient, Γ' is the projection of the curve Γ on the plane xy, and

$$P = D[C_x f_x f_y - C_y(1 + f_x^2)]/R.$$
$$Q = D[C_x(1+f_y^2) - C_y f_x f_y]/R. \tag{I.7}$$

Using Green's formula

$$\oint_{\Gamma'} P\mathrm{d}x + Q\mathrm{d}y = \int_S \int (\partial Q/\partial x - \partial P/\partial y)\mathrm{d}x\mathrm{d}y, \tag{I.8}$$

the definitions in Eq. I.7, and identity I.5, after some simple, and not too long calculations, we finally get from Eq. I.4

$$\int_S \int (C_t - D\{[C_{xx}(1 + f_y^2) + C_{yy}(1 + f_x^2) - 2C_{xy} f_x f_y]/R^2 - C_x[f_{xx} f_x(1 + f_y^2) + f_{yy} f_x(1 + f_x^2) + f_{xy}(-2f_y f_x^2)]/R^4 - C_y[f_{xx} f_y(1 + f_y^2) + f_{yy} f_y(1 + f_x^2) + f_{xy}(-2f_x f_y^2)]/R^4\}]\,\mathrm{d}x\mathrm{d}y = 0. \tag{I.9}$$

Because of the arbitrariness of S, and then of S', Eq. I.9 is equivalent to the differential equation (Eq. 2.1).

In the special case, when the surface is a plane $z = f(x,y) =$ constant, all derivatives of $f(x,y)$ vanish, and Eq. 2.1 is obviously reduced to the usual diffusion equation

$$C_t = D(C_{xx} + C_{yy}). \tag{I.10}$$

The solution of our problem in the planar case (i.e., the solution of Eq. I.10 with the initial conditions (Eq. 2.4), can be obtained analytically. That is,

$$C'(r'\,\tau) = \frac{e^{-r'^2/4\tau}}{4\tau} \sum_{k=0}^{\infty} \frac{\left(\frac{r'^2}{4\tau^2}\right)}{(k!)^2} A_k(\tau), \tag{I.11}$$

where $r' = r/r_0$, $\tau = Dt/r_0^2$, $C' = C/C_0$ and[1]

$$A_k(\tau) = \int_0^1 e^{-x/4\tau}\, x^k \mathrm{d}x = -4\tau\, e^{-1/4\tau} + 4\tau\, k\, A_{k-1}(\tau). \tag{I.12}$$

In this case the intensity of the bleached molecules can be easily evaluated as follows:

$$J_0(t) = \int_0^{r_0} 2\pi r\, C(r, t)\mathrm{d}r. \tag{I.13}$$

[1]This solution can be easily found by using, for instance, the Green function of the planar Cauchy problem of Eq. I.10 with $D=1$; that is, $G(r-r',t) = (1/4\pi t)\exp\{-(|\mathbf{r}-\mathbf{r}'|^2)/4t\}$.

By using the initial condition 2.4 we can write the solution as follows:

$$C(r,t) = C(x,y,t) = \frac{1}{4\pi t} \int_{\xi^2+\eta^2\le 1} \int \exp\left[-\frac{(x-\xi)^2 + (y-\eta)^2}{4t}\right] \mathrm{d}\xi\mathrm{d}\eta = \frac{\exp[-r^2/4t]}{4\pi t} \int_0^1 \exp[-\rho^2/4t]\, 2\pi I_0\left(\frac{r\rho}{2t}\right) \rho\, \mathrm{d}\rho$$

and by expanding the Bessel function of imaginary argument, I_0, in Taylor's series we get Eq. I.11 and I.12.

It is interesting to consider the one-dimensional case. If nothing depends on one of the coordinates (e.g., on y) Eq. 2.1 reduces to the following equation

$$C_t = D\left[\frac{C_{xx}}{1 + f_x^2} - \frac{C_x f_x f_{xx}}{(1 + f_x^2)^2}\right]. \tag{I.14}$$

Changing variable x to

$$s = \int_0^x (1 + f_x^2)^{1/2}\, \mathrm{d}x, \tag{I.15}$$

we can rewrite Eq. I.14 as was expected, in the following form,

$$C_t = D\, C_{ss}, \tag{I.16}$$

which is a usual one-dimensional diffusion equation. This result could be predicted intuitively.

APPENDIX II

Numerical Calculations

In this appendix we discuss the numerical solution of Eq. 2.1 for the surface described by Eq. 2.3. By substituting Eq. 2.3 into 2.1, we get

$$\frac{\partial C}{\partial \tau'} = \frac{C_{xx}(1 + \alpha^2\cos^2 u \sin^2 v) + C_{yy}(1 + \alpha^2\cos^2 v \sin^2 u) - 2C_{xy}\alpha^2 \sin u \cos u \sin v \cos v}{[1 + \alpha^2(\sin^2 u \cos^2 v + \sin^2 v \cos^2 u)]} - \frac{\alpha^2 k \cos u \cos v\,[2 + \alpha^2\,[(\sin^2 v + \sin^2 u)]}{[1 + \alpha^2\,(\sin^2 u \cos^2 v + \sin^2 v \cos^2 u)]^2} \cdot [C_x \cos v \sin u + C_y \cos u \sin v] \tag{II.1}$$

where

$$\alpha \equiv Ak$$
$$u \equiv kx$$
$$v \equiv ky$$
$$\tau' \equiv Dt \tag{II.2}$$

and C_x is $\partial C/\partial x$, $C_{xx} = \partial^2 C/\partial x^2$, etc.

If we denote the radius of the bleached spot by r_0, the following initial conditions exist:

$$C = \begin{cases} C_0 & x^2 + y^2 \le r_0^2 \\ 0 & x^2 + y^2 > r_0^2 \end{cases} \tag{II.3}$$

where C_0 is the initial concentration of the tagged molecules.

To express this problem in a dimensionless form, we introduce

$$x' = x/r_0 \quad y' = y/r_0 \quad \tau = Dt/r_0^2. \tag{II.4}$$

Now, Eqs. II.1 and II.3 can be rewritten in the following form:

$$\frac{\partial C}{\partial \tau} = \frac{C_{x'x'}(1 + \alpha^2 \cos^2 u \sin^2 v) + C_{y'y'}(1 + \alpha^2 \cos^2 v \sin^2 u) - 2C_{x'y'} \sin u \cos u \sin v \cos v}{[1 + \alpha^2\,(\sin^2 u \cos^2 v + \sin^2 v \cos^2 u)]} - \frac{\alpha^2 (kr_0) \cos u \cos v[2 + \alpha^2\,(\sin^2 u + \sin^2 v)]}{[1 + \alpha^2(\sin^2 u \cos^2 v + \sin^2 v \cos^2 u)]^2} \cdot [C_{x'} \cos v \sin u + C_{y'} \cos u \sin v] \tag{II.5}$$

$$C_{\tau'=0} = \begin{cases} C_0 & x'^2 + y'^2 \le 1 \\ 0 & x'^2 + y'^2 > 1 \end{cases} \qquad \text{(II.6)}$$

Eqs. II.5 and II.6 were solved numerically, using a nine-point explicit scheme (15). That is, we constructed a net with steps h along x,y and substituted in Eq. II.5 the following approximate values:

$$C_\tau \simeq \{C(jh,ih,\tau+\Delta\tau) - C(jh,ih,\tau)\}/\Delta\tau$$

$$C_{x'x'} \simeq \{C[(j+1)h,ih,\tau] - 2C(jh,ih,\tau) + C[(j-1)h,ih,\tau]\}/h^2$$

$$C_{y'y'} \simeq \{C[jh,(i+1)h,\tau] - 2C(jh,ih,\tau) + C[jh,(i-1)h,\tau]\}/h^2$$

$$C_{x'y'} \simeq \{C[(j+1)h,(i+1)h,\tau] - C[(j-1)h,(i+1)h,\tau] + C[(j-1)h,(i-1)h,\tau] - C[(j+1)h,(i-1)h,\tau]\}/4h$$

$$C_{x'} \simeq \{C[(j+1)h,ih,\tau] - C[(j-1)h,ih,\tau]\}/2h$$

$$C_{y'} \simeq \{C[jh,(i+1)h,\tau] - C[jh,(i-1)h,\tau]\}/2h. \qquad \text{(II.7)}$$

These derivatives are for a point $x=jh$ and $y=ih$ on the surface described by Eq. 2.3.

This substitution leads to a formula that expresses $C(jh,ih,\tau+\Delta\tau)$ as some function of concentration C at nine points for time τ. Because we know C for any point at $\tau=0$, we can calculate C everywhere at time $\Delta\tau$ with the help of Eq. II.7 and then, starting from time $\Delta\tau$ calculate $C(x,y)$ for time $2\Delta\tau$, and so on. The stability of this calculation scheme demands that (15)

$$\Delta\tau/h^2 \le 1/4. \qquad \text{(II.8)}$$

The interval of calculation along xy was $h=1/60$ μm and $\Delta t = r_0^2\Delta\tau/D = r_0^2/(3{,}600D)$. The intensity of the bleached molecules in the bleached spot was calculated numerically according to Eq. 2.5.

We would like to add a few words about accuracy. To avoid truncation error, calculations must be performed with "double precision" in IBM computers or with normal precision in CDC (13 digits). The analysis of cumulative errors (except these which are coming from instability) is very difficult. Some estimates can be obtained by comparison of numerical and analytical solutions in the planar case (the agreement in our calculations is better than 1%) and by changing spatial step, h. We estimate the possible errors by 5% at most.

APPENDIX III

In this Appendix we summarize some mathematical aspects of this work.

1. Let us consider membranes that can be described by the equation

$$z = f(x,y) = A\,F(x,y), \qquad \text{(III.1)}$$

where F is independent of A, and let us assume the following.

(*a*) $F(x,y)$ is such that points (x,y) which are the solutions of the equation $F(x,y) = F_0$ = constant form in our spot lines of finite length for any F_0.

(*b*) The equation $z = \eta(s) = \eta_0$ = constant (here η is the z projection of the boundary, see Eq. I.1) has a finite number of roots for any η_0. Then the following equation can be easily proved:

$$\lim_{A\to\infty} (\text{spot area}/\text{spot perimeter}) = \text{constant}, \qquad \text{(III.2)}$$

where the constant that appears in the right-hand side of Eq. III.2 is A independent. The result is true for randomly but closely distributed microvilli and for any closely packed microvilli. This result is not true if the boundary of the spot is located on the lines $z(x,y)$=constant (see, e.g., Fig. 1 *B*).

2. We would like to add a few words about k and r_0 dependence. The ratio in the right-hand side of Eq. III.2 is k dependent. However, for large enough k (for instance our k is large enough), this dependence is very weak. It is a general remark for statement *1*, and seems to be true for statement *2*. The dependence on r_0 is also predictable. The constant ratio in the right-hand side of Eq. III.2 is proportional to r_0. One can note that changes of r_0 or k are connected through scaling.

Helpful and stimulating discussions with Drs. Michael Edidin, David Wolf, Paul Dragsten, Ralph Nossal, William Hagins, Elliot Elson, and Richard Cone are greatly appreciated. The authors are grateful to Ehud Goldstein and to Calman Naftali for their helpful suggestions in programming and to the operators, Zohara Rechter and Ely Saadan for their consistent attention to our extremely long computations. The plotting of Fig. 1 by MLAB and Gary Knott are heartily acknowledged.

Received for publication 19 May 1981 and in revised form 17 November 1981.

REFERENCES

1. Frye, L. D., and M. Edidin. 1970. The rapid intermixing of cell surface antigens after formation of mouse-human heterokaryons. *J. Cell Sci.* 7:319–335.
2. Edidin, M. 1975. Rotational and translational diffusion in membranes. *Annu. Rev. Biophys. Bioeng.* 3:179–201.
3. Huang, N. W. 1973. Mobility and diffusion in the plane of cell membranes. *J. Theoret. Biol.* 40:11–16.
4. Taylor, R. B., W. P. A., Duffus, M. C. Raff, and S. de Petris. 1971. Redistribution and pinocytosis of lymphocyte surface immunoglobulin molecules induced by anti-immunoglobulin antibody. *Nat. New Biol.* 233:225–229.
5. Poo, M.-M., and R. A. Cone. 1974. Lateral diffusion of rhodopsin in the photo-receptor membrane. *Nature (Lond.).* 247:438–441.
6. Edidin, M., Y. Zagyansky, and T. J. Lardner. 1976. Measurement of membrane lateral diffusion in single cells. *Science (Wash. D.C.).* 191:466–468.
7. Schlessinger, J., P. E. Koppel, D. Axelrod, K. Jacobson, W. W. Webb, and E. L. Elson. 1976. Lateral transport on cell membranes: mobility of concanavelin A receptors on myoblasts. *Proc. Natl. Acad. Sci. U. S. A.* 73:2409–2413.
8. Wolf, D. E., J. Schlessinger, E. L. Elson, W. W. Webb, R. Blumenthal, and P. Henkart. 1977. Diffusion and patching of macromolecules on planar lipid bilayer membranes. *Biochemistry.* 16:3476–3483.
9. Smith, B. A., W. R. Clark, and H. M. McConnell. 1979. Anisotropic molecular motion on cell surfaces. *Proc. Natl. Acad. Sci. U. S. A.* 76:5641–5644.
10. Wolf, D.E., A. H. Handyside, and M. Edidin. 1982. Effect of microvilli on lateral diffusion measurements made by the fluorescence photobleaching recovery technique. *Biophys. J.* 38:295–297.
11. Aizenbud, B. and N. D. Gershon. 1980. Diffusion of molecules on biological molecules of nonplanar form. *Fed. Proc.* 39:1990.
12. Knott, G. D. 1979. MLAB. A mathematical model. *Comput. Programs Biomed.* 10:271–280.
13. Dragsten, P., P. Henkart, R. Blumenthal, J. Weinstein, and J. Schlessinger. 1979. Lateral diffusion of surface immunoglobulin, Thy-1 antigen, and a lipid probe in lymphocyte plasma membranes. *Proc. Natl. Acad. Sci. U. S. A.* 76:5163–5167.
14. Eager, D. D., M. H. Johnson, and K. W. Thurley. 1976. Ultrastructural studies on the surface membrane of mouse egg. *J. Cell Sci.* 22:345–353.
15. Berezin, I. S., and N. P. Zhidkov. 1965. Computing Methods. Vol. 2. Pergamon Press, London.